Original article

New potential AChE inhibitor candidates

A.A.N. de Paula [a,*], J.B.L. Martins [b], M.L. dos Santos [b], L. de C. Nascente [b,c], L.A.S. Romeiro [b,c], T.F.M.A. Areas [d], K.S.T. Vieira [d], N.F. Gambôa [d], N.G. Castro [d], R. Gargano [a]

[a] Instituto de Física, Universidade Brasília, CP04455, Brasília, DF, CEP 70919-970, Brazil
[b] Instituto de Química, Universidade de Brasília, CP4478, 70904-970 Brasília, DF, Brazil
[c] Pós-Graduação em Gerontologia, Universidade Católica de Brasília, QS 07 Lote 01, CEP 71966-700 Taguatinga Sul, Brasília, DF, Brazil
[d] Instituto de Ciências Biomédicas, Universidade Federal do Rio de Janeiro, Rio de Janeiro, RJ, Brazil

A R T I C L E   I N F O

A B S T R A C T

We have theoretically studied new potential candidates of acetylcholinesterase (AChE) inhibitors designed from cardanol, a non-isoprenoid phenolic lipid of cashew *Anacardium occidentale* nut-shell liquid. The electronic structure calculations of fifteen molecule derivatives from cardanol were performed using B3LYP level with 6-31G, 6-31G(d), and 6-311 + G(2d,p) basis functions. For this study we used the following groups: methyl, acetyl, *N,N*-dimethylcarbamoyl, *N,N*-dimethylamine, *N,N*-diethylamine, piperidine, pyrrolidine, and *N,N*-methylbenzylamine. Among the proposed compounds we identified that the structures with substitution by *N,N*-dimethycarbamoyl, *N,N*-dimethylamine, and pyrrolidine groups were better correlated to rivastigmine, and represent possible AChE inhibitors against Alzheimer disease.

1. Introduction

Alzheimer's disease (AD) is characterized by the progressive impairment of cognitive functions, often accompanied by behavioral disturbances [1]. Unfortunately, the causes of AD have not been completely elucidated and no disease-modifying treatment is available yet. However, the most successful approach for the symptomatic treatment of AD is based on the cholinergic hypothesis, that the cognitive deficit is a consequence of deficiency in acetylcholine (ACh) and decreased cholinergic neurotransmission [2–4].

Whitehouse et al. [5] showed that AD could also be associated with the reduction of the quantity of presynaptic nicotinic and muscarinic (M2) receptors of ACh, with retention of postsynaptic muscarinic receptors (M1 and M3) [6]. Besides ACh, Storga et al. [7] and Coyle et al. [8] verified that the levels of other neurotransmitters, such as serotonin, noradrenaline, dopamine, glutamate and substance P, are significantly reduced. The effects of ACh are terminated by acetylcholinesterase (AChE), which hydrolyzes ACh via an acylenzyme mechanism that involves nucleophilic (serine) and general acid base (histidine) elements [9–11]. Thus an AChE inhibitor (AChEI) may improve cholinergic neurotransmission and

could be used as a natural therapeutic strategy in order to attenuate the cognitive deficit in AD [3,4,12,13]. Therefore, several experimental and theoretical methods have been applied to study acetylcholinesterase, as well as novel candidate AChEIs [14–19].

Anticholinesterasic compounds such as tacrine and donepezil, as well as the alkaloids galantamine, physostigmine, huperzine and acetyl-spectaline showed promising activity for AD treatment [20]. Another centrally acting and slowly reversible cholinesterase inhibitor, called rivastigmine, was approved for AD by the FDA [20]. Rivastigmine increases the concentration of ACh through a long-lasting carbamoylation of acetylcholinesterase, enhancing cholinergic function.

In searching for new compounds useful for AD treatment, we designed new candidate AChEIs from non-isoprenoid phenolic lipids (NIPLs) of *Anacardium occidentale* [21]. Anacardic acids, cardols, cardanols and methylcardols are the main NIPL components of the cashew nut-shell liquid (CNSL) and have been used for potential bioactive compounds generation [22–24]. The phenolic lipid derivatives have electronic, structural and hydrophobic characteristics relevant for the molecular recognition of AChE. In a recent work [21] we have compared the electronic properties (HOMO, LUMO, HOMO − 1, LUMO − 1, energies and derived values) of modified phenolic lipids against rivastigmine, using semi-empirical and RHF methods. The molecular pattern used involves the hybridization between the primary pharmacophoric subunit of rivastigmine and the secondary subunit of an alkyl side chain of acetyl-spectaline.

* Corresponding author. Tel.: +55 61 3307 2900; fax: +55 61 3307 2363.
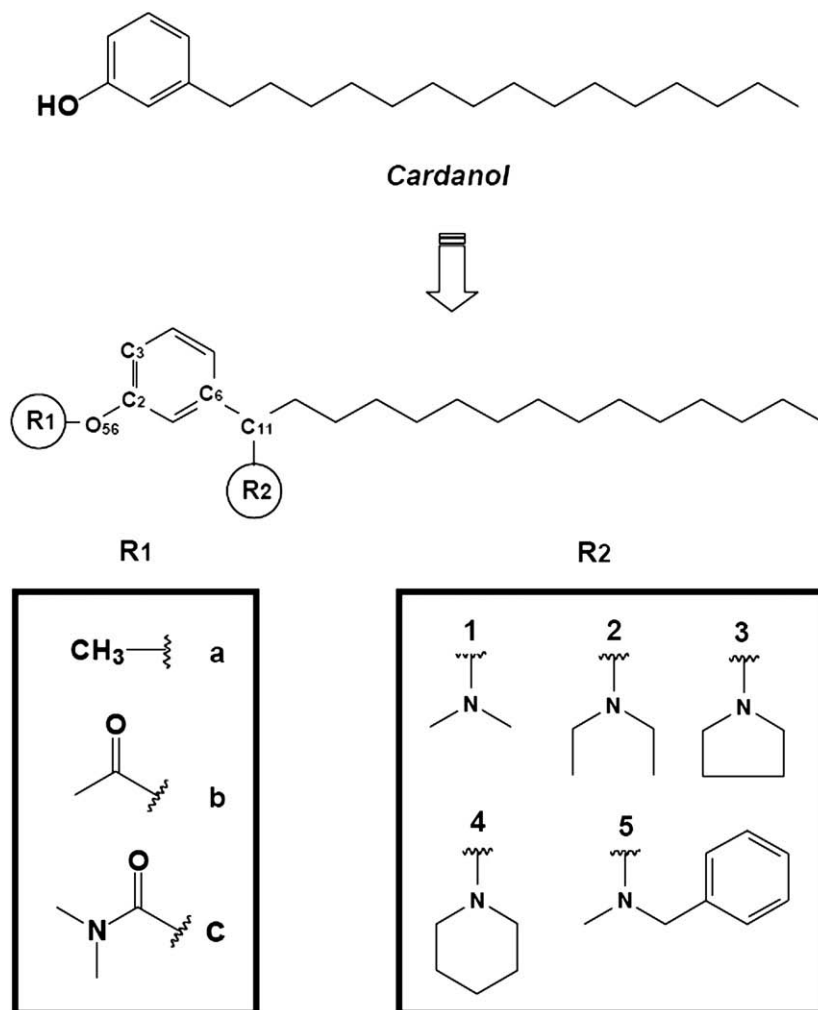E-mail address: anevesfisica@yahoo.com.br (A.A.N. de Paula).

Fig. 1. Schematic representation and notation used for the compound series obtained from the cardanol pattern with substitution of R1 and R2 groups.

In the present study new properties were included, e.g., charge of aromatic ring, carbon and nitrogen, using B3LYP level with 6-31G, 6-31G(d), and 6-311 + G(2d,p) basis functions. These properties, taking into account correlation effects, were used in the Principal Components Analysis (PCA), a multivariate statistical method [25]. In order to improve this analysis, the PCs were obtained in a three-dimensional PCA model. Therefore, these B3LYP results complement our previous study [21]. Furthermore, these results could improve the knowledge of important properties for AChE inhibition.

This paper is organized as follows. In Section 2, we present the methodologies for the electronic property calculations of CNSL phenolic lipid derivatives and for the three-dimensional PCA in order to correlate with the rivastigmine structure. The results and their discussion are given in Section 3. In Section 4 we present the main conclusions.

2. Methodologies

We have recently [21] proposed a new set of AChEI molecules based on the substitution of hydrogen from the phenolic group of cardanol (R1 in Fig. 1) by groups such as (a) methyl, (b) acetyl, and (c) N,N-dimethylcarbamoyl, as well as substitutions at the benzylic carbon from the side chain (R2 in Fig. 1) by secondary amines, e.g., (1) N,N-dimethylamine, (2) N,N-diethylamine (3) pyrrolidine,
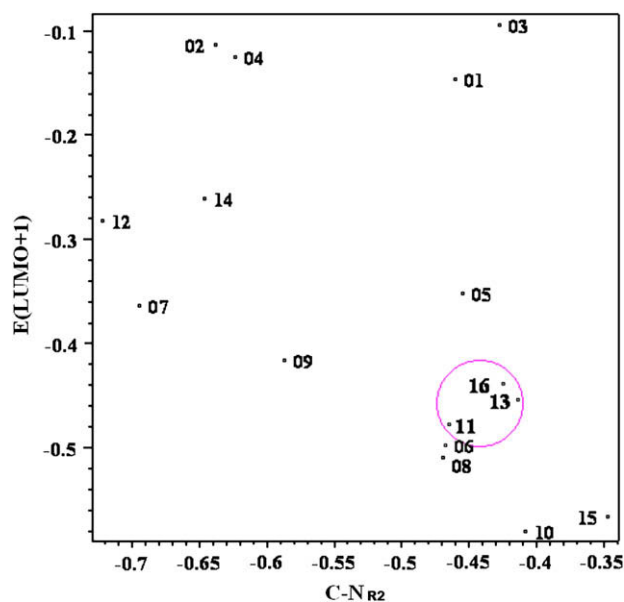

Fig. 2. Contribution of E(LUMO + 1) versus C–N$_{R2}$ for the cardanol derivatives and rivastigmine.

Table 1

Notation used for the substitution of hydrogen from the phenolic group of cardanol (R1 in the Fig. 1) and benzylic carbon from the side chain (R2 in the Fig. 1). CA stands for cardanol.

Compound number	Structure
01	CA_a_1
02	CA_a_2
03	CA_a_3
04	CA_a_4
05	CA_a_5
06	CA_b_1
07	CA_b_2
08	CA_b_3
09	CA_b_4
10	CA_b_5
11	CA_c_1
12	CA_c_2
13	CA_c_3
14	CA_c_4
15	CA_c_5
16	Rivastigmine

(4) piperidine, and (5) N,N-methylbenzylamine. The variations obtained from the substitutions yielded fifteen structures of cardanol derivatives. Table 1 shows the notation used for the cardanol derivative compounds used in this work.

Geometries of these fifteen structures as well as rivastigmine were taken from the optimized results [21] using the semi-empirical AM1 and PM3 methods. Conformational analysis of minimum energy was performed using the potential energy surface maps (Fig. 3 of Ref. [21]). These minimum structures were fully optimized and the procedures for this study used the following steps:

- The single point electronic property calculations, i.e., energies of the two highest occupied molecular orbitals E(HOMO) and E(HOMO − 1), energies of the two lowest unoccupied molecular orbitals E(LUMO) and E(LUMO + 1), charge of aromatic ring (see Fig. 1 for the notation), charge of C_{11} (C–C_{11}), charge of O_{56} (C–O_{56}) and charge of nitrogen belonging to R2 group (C–N_{R2}) were performed using B3LYP method with the following basis sets: 6-31G, 6-31G(d) and 6-311 + G(2d,p).
- From these electronic data we next derived the GAP [E(LUMO) − E(HOMO)], GAP + 1 [E(LUMO + 1)–E(HOMO − 1)], ΔH-1 [E(HOMO) − E(HOMO − 1)] and ΔL + 1 [E(LUMO + 1) − E(LUMO)] properties.

The calculations were carried out using Gaussian03 computational program [26].

In order to compare the electronic properties obtained from the fifteen cardanol derivatives with rivastigmine, we have used PCA. This method reduces the initial parameter set (electronic properties) to the most relevant ones regarding the ability to select compounds that are more similar to rivastigmine. The PCA data were auto scaled using the average values of each electronic property as zero and the related standard deviation as unit. This procedure was used in order to eliminate artificial effects, where some electronic properties with large values could dominate the analysis. The next step was to analyze each property of fifteen derivatives with the aim of selecting compounds that most resemble rivastigmine. We have also analyzed pairs of electronic property relationships among the fifteen compounds. This last analysis was important to yield the most relevant variables in relation to rivastigmine. For example, Fig. 2 shows the contribution of E(LUMO + 1) versus C–N_{R2} for the cardanol derivatives and rivastigmine. From these preliminary data, the electronic variables used for the PCA calculation were modified and then classified into
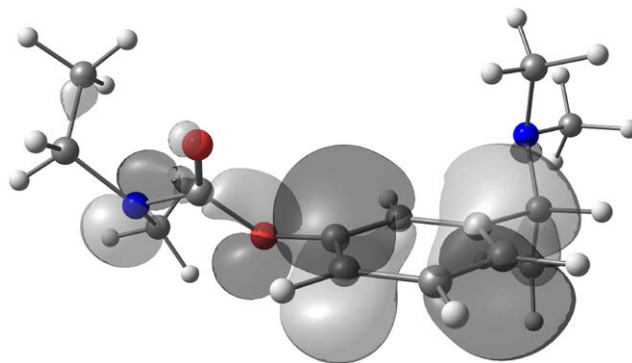

Fig. 3. Optimized geometry of rivastigmine. The HOMO − 1 orbital of rivastigmine at B3LYP/6-311 + G(2d,p) level is also shown.

the principal components (PCs) in order of significance. The first component is a linear combination of electronic properties with the highest variance of data in relation to the others.

3. Results and discussion

The values for the studied properties taken from the fifteen structures were very close for all basis sets considered. Consequently, throughout the text we have reported only the most extended basis set 6-311 + G(2d,p) in order to better represent the final results.

The HOMO − 1 orbital of rivastigmine at B3LYP/6-311 + G(2d,p) level using AM1 optimized geometry (Fig. 3) shows a main contribution from the π orbital of the aromatic ring. The same contribution of HOMO − 1 orbital is found for all calculated structures, i.e., the contributions are centered mainly in the fragment analogous to rivastigmine for all compounds.

Table 2 presents the results of HOMO − 1, HOMO, LUMO and LUMO + 1 energies, and also the charge of benzyl ring, C_{11}, O_{56}, and N_{R2} of cardanol derivatives and rivastigmine.

A systematic study was performed considering binary analysis of all properties, PC variance and weight of the calculated electronic data. Fig. 2 shows the E(LUMO + 1) versus C–N_{R2} for the CA_c_1 and

Table 2

Electronic structure values for E(HOMO − 1), E(HOMO), E(LUMO), E(LUMO + 1), charge for ring, C–C_{11}, C–O_{56} and C–N_{R2} of fifteen compounds derived from cardanol and rivastigmine (**16**).

	Orbital energies (eV)				Charge			
	HOMO − 1	HOMO	LUMO	LUMO + 1	Ring	C_{11}	O_{56}	N_{R2}
01	−6.13	−5.74	−0.37	−0.15	0.20	0.35	−0.38	−0.46
02	−6.16	−5.45	−0.38	−0.11	0.22	0.15	−0.36	−0.64
03	−6.18	−5.43	−0.40	−0.09	0.29	−0.08	−0.35	−0.43
04	−6.11	−5.50	−0.35	−0.12	0.21	0.31	−0.38	−0.62
05	−6.11	−5.77	−0.49	−0.35	0.04	0.40	−0.35	−0.45
06	−6.77	−5.81	−0.55	−0.50	0.28	0.41	−0.54	−0.47
07	−6.50	−5.81	−0.78	−0.36	0.27	0.33	−0.52	−0.70
08	−6.83	−5.53	−0.56	−0.51	0.35	0.15	−0.54	−0.47
09	−6.67	−5.54	−0.50	−0.42	0.29	0.35	−0.54	−0.59
10	−6.80	−5.87	−0.59	−0.58	0.34	0.31	−0.54	−0.41
11	−6.76	−5.80	−0.49	−0.48	0.21	0.48	−0.43	−0.46
12	−6.62	−5.56	−0.34	−0.28	0.19	0.46	−0.45	−0.73
13	−6.78	−5.45	−0.51	−0.45	0.34	−0.10	−0.44	−0.42
14	−6.59	−5.50	−0.39	−0.26	0.21	0.26	−0.44	−0.65
15	−6.67	−5.69	−0.61	−0.57	0.33	0.05	−0.43	−0.35
16	−6.64	−5.99	−0.49	−0.44	0.19	0.33	−0.39	−0.42

CA_c_3 cardanol derivatives (Table 1) that most resemble rivastigmine.

Initially, we have used the properties of all structures in the PC analysis. Then we have excluded some of the properties from this analysis trying to find their relevance. This allowed us to find the three most significant properties divided into three cases, named cases I, II and III (Fig. 4). We identified that the descriptors E(HOMO − 1), E(LUMO + 1) and C–O_{56} are common to the three cases. They appeared to be the main properties for a good clustering among the structures best correlated to rivastigmine. Besides these

properties we also identified C–N_{R2}, used in cases I and III, LUMO, used in cases II and III, and ΔL + 1, used in case II, as suitable descriptors. Table 3 presents the variance of each component (PC1, PC2, and PC3), with its respective percentage. In case II we had the highest percent value for PC1 and we had the best percent of cumulative variance, nearly 97.5%, for the first three PCs in cases I and II. Table 4 shows the weights of the most significant properties for the first three PCs. We found from the PCA analysis (Fig. 4) that the structures that are best correlated to rivastigmine are the dimethylcarbamates **11** (CA_c_1) and **13** (CA_c_3) for all three cases
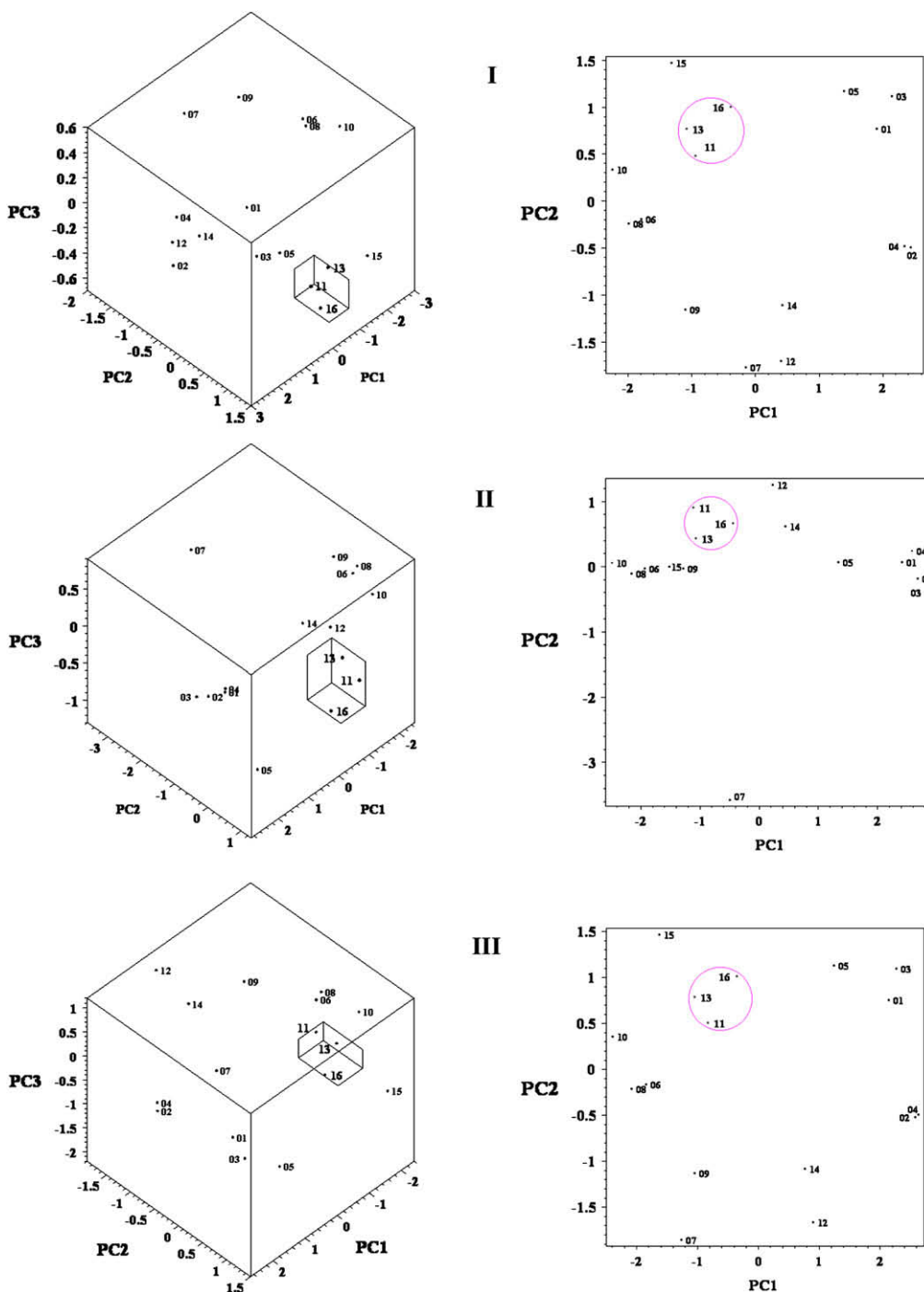

Fig. 4. Score plots of sets I, II, and III obtained from the PCA, showing the separation of cardanol derivatives and rivastigmine.

Table 3
Variance, percent and cumulative in cases I, II and III of PC1, PC2 and PC3 obtained with PCA.

	Case I			Case II			Case III		
	Variance	Percent	Cumulative	Variance	Percent	Cumulative	Variance	Percent	Cumulative
PC1	39.35	65.59	65.59	51.00	68.00	68.00	47.01	62.68	62.68
PC2	16.48	27.47	93.06	16.46	21.95	89.95	16.50	22.00	84.68
PC3	2.65	4.41	97.47	5.87	7.82	97.77	8.13	10.84	95.52

studied. These results indicated the substituents most likely to yield promising candidates to the development of AChE inhibitors for the treatment of AD from cardanol.

The predictions of the analysis were then evaluated experimentally for the series of dimethylcarbamates **11**–**15**. The compounds were synthesized from cardanol as hydrochlorides, using standard methods. Enzyme inhibition was assayed as previously described [31], except that purified AChE from *Electrophorus electricus* was used instead of tissue homogenates. Compounds **11**–**13** inhibited AChE in a concentration-dependent manner (Fig. 5), while **14** and **15** showed little activity, inhibiting the enzyme by less than 25% at 100 μM. The dimethylamino **11** was the most potent, with an IC_{50} of 50.0 μM, followed closely by the pyrrolidinyl **13** (84.3 μM) and the diethylamino **12** (251.1 μM). Thus, the PCA procedure correctly selected the two most potent compounds in the series.

According to the literature [27–29] rivastigmine reaches the bottom of the active-site gorge where it interacts with the Ser200 residue of the catalytic triad Ser200-His440-Glu327 through its carbamoyl moiety while the aromatic and the ammonium groups are addressed to interact with the conserved residue Trp84 (adjacent to the catalytic triad) and a second aromatic residue, Phe330, which seems to be involved in cation-π aromatic or hydrophobic interactions. By a common mechanism of inhibition, the carbamoyl group is covalently linked to the active-site serine, while the leaving group, (−)-S-3-[1-(dimethylamino)-ethyl]phenol (NAP), itself a competitive AChE inhibitor, remains in the active-site gorge. Bar-On and co-workers demonstrated that phenol group of NAP is within hydrogen bonding distance to interact with the backbone of the Gly118 residue, while aromatic and methyl groups make hydrophobic–aromatic and π–π interactions with Trp84 and Phe330 [27].

Considering the possibility that the cardanol derivatives are able to penetrate deeply until reaching the bottom of the active-site gorge in the same way of rivastigmine and taking into account the results previously described by Sterling and co-workers [30] that showed a 30-fold higher AChEI activity of the N,N-dimethylcarbamoyl analogue of rivastigmine in comparison with the N,N-ethyl-methylcarbamoyl moiety, we expect a better access of the Ser200 residue to the N,N-dimethylcarbamoyl moiety of CA_c_1 (**11**) and CA_c_3 (13) resulting in the carbamoylation of this residue. In order to evaluate the influence of the hydrophobic contribution as well as conformational freedom of the ammonium

moiety, the dimethylamine (**11**) and its conformationally constrained bis-homologue pyrrolidine (**13**) groups were selected. In this case, the increase of a hydrophobic region in the pyrrolidine is expected to interact with the Trp84 and Phe330 residues better than dimethylamine, unless there is a steric restriction in the adjacent catalytic triad region delimiting the volume accessible to the pyrrolidinium group. Concerning the long aliphatic side chain, we expected it to accommodate along the gorge, where there are possible interactions with complementary hydrophobic/aromatic aminoacid residues.

On the other hand, Castro and co-workers [31] using flexible docking experiments pointed out that derivatives of the natural piperidine alkaloid (−)-spectaline were not likely to interact with the active-site triad, possibly due to the volume of long aliphatic side chains. In a similar manner, if the volumes of the long aliphatic side chain of CA_c_1 (**11**) and CA_c_3 (**13**) do not allow the derivatives to reach the bottom of the active site, they might be able to interact similarly to spectaline or even donepezil [15] by cation–π and π–π aromatic interactions of the ammonium groups and the aromatic moiety with the aromatic residue Phe330, Trp84 halfway up the active-site gorge or Trp279 at the peripheral anionic site (PAS), while hydrogen bonds are expected to occur with ammonium and carbamate groups from the backbone of the aromatic and hydrophobic and hydrogen bond donors at the PAS residues, e.g., Tyr70, Tyr121 and Trp279, and Phe288, Phe290, Phe331, Arg289 and Ser286 above the PAS at the top of the gorge as well as water molecules [15]. Since the walls of the gorge are lined predominantly by aromatic residue side chains, hydrophobic interactions from the long aliphatic chain of these cardanol derivatives are expected to be a significant contribution in the recognition by AChE and modulation of their activities.

Table 4
Weight of electronic properties $E(HOMO − l)$, $E(LUMO + 1)$, $C–O_{56}$, $C–N_{R2}$, $E(LUMO)$ and $\Delta L + 1$ of PC1, PC2 and PC3 in cases I, II and III, obtained with PCA.

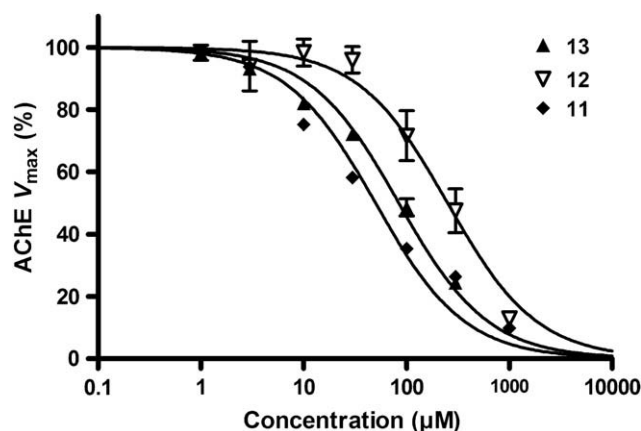|	Case I			Case II			Case III		
	PC1	PC2	PC3	PC1	PC2	PC3	PC1	PC2	PC3
$E(HOMO − l)$	0.58	0.12	0.61	0.51	−0.15	−0.22	0.50	0.10	−0.52
$E(LUMO + 1)$	0.59	−0.17	0.13	0.52	−0.04	0.44	0.54	−0.18	−0.10
$C–O_{56}$	0.51	0.44	−0.72	0.46	0.23	−0.74	0.47	0.43	−0.09
$C–N_{R2}$	−0.23	0.87	0.30				−0.20	0.88	0.05
$E(LUMO)$				0.36	0.66	0.43	0.44	0.03	0.84
$\Delta L + 1$				0.36	−0.69	0.18			

Fig. 5. Acetylcholinesterase inhibiton curves for selected cardanol derivatives. Symbols are means ± SD (n = 3) of *E. electricus* AChE maximum reaction velocity (V_{max}) relative to control (without inhibitor). The solvent had negligble effects at the concentrations tested. The lines depict the regression function for the standard single-site complete inhibition model.

4. Conclusions

The aim of this work was to investigate newly designed candidates AChE inhibitors based on cardanol derivatives using a multivariate analysis.

For the achievement of our purpose we have used the B3LYP method with the 6-31G, 6-31G(d) and 6-311 + G(2d,p) basis functions. Final results were reported using the extended 6-311 + G(2d,p) basis set. The analyses of the proposed structures were performed by pairs in order to find the main descriptors, based on the correlation with rivastigmine. The most relevant electronic properties emerging from the PCA were $E(HOMO-1)$, $E(LUMO+1)$, $C-O_{56}$, $C-N_{R2}$, $E(LUMO)$ and $\Delta L+1$.

The PCA also showed that compounds **11** and **13** are better correlated to rivastigmine. The analyses predicted a possible activity of these compounds as inhibitors of AChE and this was confirmed by synthesis and phamacological testing. Efforts to further clarify the mechanism of enzyme inhibition of these compounds are currently under way.

Acknowledgments

References

[1] P.T. Francis, A.M. Palmer, M. Snape, G.K. Wilcock, J. Neurol. Neurosurg. Psychiatry 66 (1999) 137–147.
[2] R.T. Bartus, R.L. Dean III, B. Beer, A.S. Lippa, Science 217 (1982) 408–414.
[3] G. Benzi, A. Moretti, Eur. J. Pharmacol. 346 (1998) 1–13.
[4] E. Giacobine, R. Becker, Cholinesterase Inhibitors do More Than Inhibit Cholinesterase, in: Alzheimer's Disease: Molecular Biology to Therapy, Birrkhayser, Boston, 1997.
[5] P.J. Whitehouse, A.M. Martion, K.A. Marcus, Arch. Neurol. 45 (1998) 722–724.
[6] A. Nordberg, I. Alafuzoff, B. Winblad, J. Neurosci. Res. 31 (1992) 103–111.
[7] D. Storga, K. Vrecko, J.G. Birkmayer, G. Reinnegger, Neurosci. Lett. 203 (1996) 29–32.
[8] J.T. Coyle, D.L. Price, M.R. Delong, Science 219 (1983) 1184–1190.
[9] D.M. Quinn, Chem. Rev. 87 (1987) 955–979.
[10] J.L. Sussman, M. Harel, F. Frolow, C. Oefner, A. Goldman, L. Toker, I. Silman, Science 253 (1991) 872–879.
[11] T.K. Manojkumar, C.Z. Cui, K.S. Kim, J. Comput. Chem. 26 (2005) 606–611.
[12] H. Sugimoto, Y. Yamanishi, Y. Iimura, Y. Kawakami, Curr. Med. Chem. 7 (2000) 303–339.
[13] N.C. Inestrosa, M.C. Dinamarca, A. Alvarez, FEBS J. 275 (2008) 625–632.
[14] Y. Paukku, A. Michalkova, D. Majumdar, J. Leszczynski, Chem. Phys. Lett. 422 (2006) 317–322.
[15] C.Y. Niu, Y.C. Xu, Y. Xu, X.M. Luo, W.H. Duan, I. Silman, J.L. Sussman, W.L. Zhu, K.X. Chen, J.H. Shen, H.L. Jiang, J. Phys. Chem. B 109 (2005) 23730–23738.
[16] S. Kone, N. Galland, J. Graton, B. Illien, C. Laurence, C. Guillou, J.Y. Le Questel, Chem. Phys. 328 (2006) 307–317.
[17] H.F. Ji, H.Y. Zhang, Theochem-J. Mol. Struct. 767 (2006) 3–9.
[18] C. da Silva, V.L. Campo, I. Carvalho, C.A. Taft, J. Mol. Graphics 25 (2006) 169–175.
[19] I. Correia, N. Ronzani, N. Platzer, B.T. Doan, J.C. Beloeil, J. Phys. Org. Chem. 19 (2006) 148–156.
[20] G. Orhan, I. Orhan, B. Sener, Lett. Drug Des. Discov. 3 (2006) 268–274.
[21] A.A.N. de Paula, J.B.L. Martins, R. Gargano, M.L. dos Santos, L.A.S. Romeiro, Chem. Phys. Lett. 446 (2007) 304–308.
[22] M.L. Dos Santos, G.C. De Magalhaes, J. Braz. Chem. Soc. 10 (1999) 13–20.
[23] I.S. Resck, M.L. Dos Santos, L.A.S. Romeiro, Heterocycles 65 (2005) 311–318.
[24] L.P.L. Logrado, M.L. Dos Santos, D. Silveira, L.A.S. Romeiro, M.O. Moraes, B.C. Cavalcanti, L.V. Lotufo, C.O. Pessoa, J. Braz. Chem. Soc. 16 (2005) 1217–1225.
[25] C. Chatfield, J. Collins, Introduction to Multivariate Analysis, Cambrigde University Press, Cambridge, 1980.
[26] M.J. Frisch, G.W. Trucks, H.B. Schlegel, G.E. Scuseria, M.A. Robb, R.J. Cheeseman, J.A. Montgomery, T.V. Jr, K.N. Kudin, J.C. Burant, J.M. Millam, S.S. Iyengar, J. Tomasi, V. Barone, B. Mennucci, M. Cossi, G. Scalmani, N. Rega, G.A. Petersson, H. Nakatsuji, M. Hada, M. Ehara, K. Toyota, R. Fukuda, J. Hasegawa, T.N.M. Ishida, Y. Honda, O. Kitao, M.K.H. Nakai, X. Li, J.E. Knox, H.P. Hratchian, J.B. Cross, C.A.V. Bakken, J. Jaramillo, R. Gomperts, R.E. Stratmann, A.J.A.O. Yazyev, R. Cammi, C. Pomelli, J.W. Ochterski, K.M.P.Y. Ayala, G.A. Voth, P. Salvador, J.J. Dannenberg, S.D.V.G. Zakrzewski, A.D. Daniels, M.C. Strain, D.K.M.O. Farkas, A.D. Rabuck, K. Raghavachari, J.V.O.J.B. Foresman, Q. Cui, A.G. Baboul, S. Clifford, B.B.S.J. Cioslowski, G. Liu, A. Liashenko, P. Piskorz, R.L.M.I. Komaromi, D.J. Fox, T. Keith, M.A. Al-Laham, A.N.C.Y. Peng, M. Challacombe, P.M.W. Gill, W.C.B. Johnson, M.W. Wong, C. Gonzalez, J.A. Pople, Gaussian03, Revision D.01, Gaussian, Inc., Wallingford CT, 2004.
[27] P. Bar-On, C.B. Millard, M. Harel, H. Dvir, A. Enz, J.L. Sussman, I. Silman, Biochemistry 41 (2002) 3555–3564.
[28] C. Bartolucci, M. Siotto, E. Ghidini, G. Amari, P.T. Bolzoni, M. Racchi, G. Villetti, M. Delcanale, D. Lamba, J. Med. Chem. 49 (2006) 5051–5058.
[29] S. Darvesh, K.V. Darvesh, R.S. McDonald, D. Mataija, R. Walsh, S. Mothana, O. Lockridge, E. Martin, J. Med. Chem. 51 (2008) 4200–4212.
[30] J. Sterling, Y. Herzig, T. Goren, N. Finkelstein, D. Lerner, W. Goldenberg, I. Miskolczi, S. Molnar, F. Rantal, T. Tamas, G. Toth, A. Zagyva, A. Zekany, G. Lavian, A. Gross, R. Friedman, M. Razin, W. Huang, B. Krais, M. Chorev, M.B. Youdim, M. Weinstock, J. Med. Chem. 45 (2002) 5260–5279.
[31] N.G. Castro, R.S. Costa, L.S.B. Pimentel, A. Danuello, N.C. Romeiro, C. Viegas Jr., E.J. Barreiro, C.A.M. Fraga, V.S. Bolzani, M.S. Rocha, Eur. J. Pharm. 580 (2008) 339–349.